Structural Engineering and Mechanics, *Vol. 67, No. 2 (2018) 115-123*
DOI: https://doi.org/10.12989/sem.2018.67.2.115

The critical buckling load of reinforced nanocomposite porous plates

Habib Guessas[1], Mohamed Zidour*[2,3], Mustapha Meradjah[1] and Abdelouahed Tounsi[1,4]

[1]*Laboratory of Matérials et Hydrology, University of Sidi Bel Abbés, BP 89 Cité Ben M'hidi, 22000 Sidi Bel Abbés, Algeria*
[2]*Université Ibn Khaldoun, BP 78 Zaaroura, 14000 Tiaret, Algeria*
[3]*Laboratory of Geomatics and Sustainable Development, Ibn Khaldoun University of Tiaret, Algeria*
[4]*Department of Civil and Environmental Engineering, King Fahd University of Petroleum & Minerals, 31261 Dhahran, Eastern Province, Saudi Arabia*

(Received March 16, 2018, Revised April 19, 2018, Accepted April 21, 2018)

Abstract. By using the first order shear deformation plate theory (FSDT) in the present paper, the effect of porosity on the buckling behavior of carbon nanotube-reinforced composite porous plates has been investigated analytically. Two types of distributions of uniaxially aligned reinforcement material are utilized which uniformly (UD-CNT) and functionally graded (FG-CNT) of plates. The analytical equations of the model are derived and the exact solutions for critical buckling load of such type's plates are obtained. The convergence of the method is demonstrated and the present solutions are numerically validated by comparison with some available solutions in the literature. The central thesis studied and discussed in this paper is the Influence of Various parameters on the buckling of carbon nanotube-reinforced porous plate such as aspect ratios, volume fraction, types of reinforcement, the degree of porosity and plate thickness. On the question of porosity, this study found that there is a great influence of their variation on the critical buckling load. It is revealed that the critical buckling load decreases as increasing coefficients of porosity.

Keywords: nanotubes; buckling; shear deformation; porosity; plate

1. Introduction

In 1991, Iijima published a paper in which they described The Helical microtubules of graphitic carbon two years later, Iijima and Ichihashi (1993) reported a Single-shell carbon nanotube of 1 nm diameter. A short time ago, several studies investigating (CNTs) have been carried, indicated that the carbon nanotubes (CNTs) their high elastic modulus, mechanical properties and low density (Pradhan and Phadikar 2009, Kolahchi *et al.* 2016b), Although several studies on the nonlocal behavior of CNTs have been carried out based on beam model theory (Zidour *et al.* 2012, Chemi *et al.* 2015, Rakrak *et al.* 2016).

The continuum mechanics methods are widely used to predict the responses of Visco and piezoelectric nano beam and nano plates (Kolahchi *et al.* 2017a, Kolahchi *et al.* 2016a, Kolahchi *et al.* 2016c, Shokravi 2017, Bellifa *et al.* 2017a, Besseghier *et al.* 2017, Behrouz Karami *et al.* 2018a, Karami *et al.* 2018b, Bouazza *et al.* 2015b). In another hand, the continuum mechanics methods are used to analyze the micro-composite system such as, buckling (Bellifa *et al.* 2017b), static and free vibration (Hebali *et al.* 2014, Ait Amar Meziane *et al.* 2014, Bouhadra *et al.* 2018), Bending analysis (Bousahla *et al.* 2014, Zidi *et al.* 2014), thermal stability and Hygrothermo-mechanical (Bousahla *et al.* 2016, Beldjelili *et al.* 2016, Attia *et al.* 2018), More recent attention has focused on mechanical response, buckling, free vibration, etc. of FGM structural elements (Belabed *et al.* 2018, El-Haina *et al.* 2017, Menasria *et al.* 2017, Bennoun *et al.* 2016, Bouderba *et al.* 2016, Bouazza *et al.* 2015a). During the last two decade there has been a considerable research reports on the carbon nanotube-reinforced polymer composite investigated that they have good properties to produce high multifunctional composites and performance structural for various potential applications. Ajayan *et al.* (1994) have considered nano-composites made from polymer reinforced by aligned CNT arrays. In recent years, has focused on the behaviour of concrete columns reinforced with nano-particles (Arani and Kolahchi 2016, Bilouei *et al.* 2016, Shokravi 2017c, Zamanian *et al.* 2017, Zarei *et al.* 2017)

Recently, a variety theoretical, experimental and computer simulation study are used carbon nanotubes (CNTs) for reinforcing nano-composite structures such as bending, buckling and vibration responses of functionally graded carbon nanotube-reinforced composite (Shafiei *et al.* 2017, Moradi-Dastjerdi 2016), embedded FG-SWCNT-reinforced microplates (Kolahchi *et al.* 2015). Thermomechanical properties of nanocomposites (Fidelus *et al.* 2005) FG-CNT-reinforced sandwich plates (Kolahchi *et al.* 2017b) and Thermoelastic analysis of CNT reinforced functionally graded sandwich structure (Mehar *et al.* 2017).

However, composite manufacturing processes are complex and can lead to the appearance or development of defects such as porosity, which affect the mechanical properties of the structure. Porosity defect is defined by the presence of small cavities which contains gaseous matter, which are called pores and which are categorized according to their size (micro, méso and macro-pores), this defect is due to improper air extraction due to various parameters

*Corresponding author, Ph.D.
E-mail: zidour.m@univ-tiaret.dz

ISSN: 1225-4568 (Print), 1598-6217 (Online)

such as viscosity of the matrix, vacuum pressure or humidity when storing the material.

Liu *et al.* (2006) also gave the discussion on effects of cure cyles on void content and mechanical properties of composites laminates. Costa *et al.* (2001) investigated the influence of porosity on the ILSS of carbon/epoxy and carbon/bismaleimide fabric laminates. A recent study by Madsen *et al.* (2003) involved the influence of porosity on physical properties of unidirectional plant fibre composites. In another study, found the effect of porosity on mechanical response of functionally graded beams with and without elastic foundations (Ait Atmane *et al.* 2015, Ait Yahia *et al.* 2015).

The presence of porosity in composite parts is an inevitable fact. Thus, limits were fixed according to the applications: in the aerospace structures working dynamically, a rate of porosities exceeding 1% is not tolerable (Liu *et al*. 2006); unlike others applications where a level of 5% or more can be tolerated (Ghiorse 1993) in the present analysis for fully isolated pores of nearly spherical or elliptical shape a rate of porosities used don't exceeded 4%.

Due to difficulties encountered in experimental methods, different authors have used the continuum mechanics methods to investigate the behaviour of micro and nano structures (Tounsi *et al*. 2015, Shokravi 2017, Belabed *et al*. 2014, Tounsi *et al*. 2016).

Porous polymers and polymer foams have unique characteristics which can be exploited in a variety of applications, such as drug delivery, (Nam and Park 1999), liquid/gaseous separation, (Ulbricht 2006) low-κ dielectrics for microelectronics. (Vora *et al.* 2001) fabrication of cushions or coatings for micro-electro-mechanical systems, (Xu *et al.* 1999) super hydrophobic coatings, (Levkin *et al.* 2009) membrane oxygenators, (Iwasaki *et al.* 2002) acoustic dampers, (Verdejo *et al.* 2009). For these applications, analyzes of the behaviour of polymer with porosity is important, because the increase of porosity is usually accompanied by variations in the mechanical properties of the polymer.

The superlative properties of carbon nanotubes, make it an excellent reinforcement for polymer matrix. This view is supported by Wan *et al.* (2005) who analyzed the effective moduli of the CNT reinforced polymer composite, with emphasis on the influence of CNT length and CNT matrix interphase on the stiffening of the composite. On the other hand, the functionally graded Distributions of carbon nanotube titled (FG-CNT) along the thickness direction has been widely investigated in the current years (Lei *et al*. 2013, Mehar *et al*. 2017, Shen 2009, Kolahchi *et al.* 2016, Hamid Madani *et al.* 2016, Kolahchi and Cheraghbak 2017, Kolahchi *et al.* 2017, Mohammad Hadi Hajmohammad *et al.* 2017). Maryam Shokravi (2017a) analyzed the buckling of sandwich plates with FG-CNT-reinforced layers resting on orthotropic elastic medium using Reddy plate theory. Reza Kolahchi *et al.* (2017) optimized in the resent paper, the dynamic buckling for sandwich nanocomposite plates with sensor and actuator layer based on sinusoidal-visco-piezoelasticity theories using Grey Wolf algorithm.

This present paper attempts to show the effects of porosity on the buckling problems of CNTRC plates using the shear deformation plate theory. With simply supported CNTRC, this research seeks to analyze the influences of various parameters on the critical buckling load of plates such as plate thickness, aspect ratios, volume fraction of CNTs and sandwich plate types and the percentage of porosity.

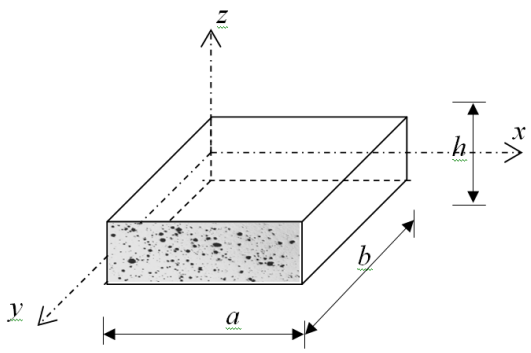

Fig. 1 Geometries of reinforced plate with porosity

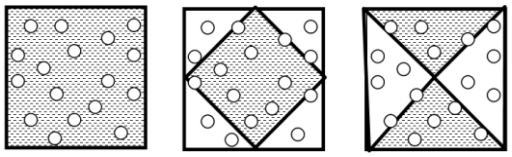

Fig. 2 Cross sections with different type of carbon nanotube reinforcement with porosity

2. Geometrical and properties of reinforced plate with porosity

As shown in Figs. 1 and 2, The proposed model is a reinforced plate referring to coordinates (x, y, z) with length a, width b and thickness h. In this investigation, the top and bottom faces of the plate are at z=±h/2.

The proposed plate with porosity is reinforced by four different types of aligned carbon nanotube distribution of across the plate thickness. The UD-CNT plate represents the uniform distribution and O-CNT, X-CNT plate are the functionally graded symmetrical distribution of CNTs.
Within the area the density of CNTs is constant, and the volume fraction varies through the thickness of the plate.

In the present study, according to the rule of mixture of CNTs and an isotropic polymer Esawi scheme (2007) by introducing the CNT efficiency parameters (η_1, η_2, η_3), the effective Young's modulus and shear modulus of CNTRC layer can be expressed as (Shen 2009)

$$E_{11} = \eta_1 V_{cnt} E_{11}^{cnt} + V_p E^p \tag{1a}$$

$$E_{22} = \eta_2 \frac{E_{22}^{cnt} E^p}{V_p E_{22}^{cnt} + V_{cnt} E^p} \tag{1b}$$

$$G_{12} = \eta_3 \frac{G_{12}^{cnt} G^p}{V_{cnt} G^p + V_p G_{12}^{cnt}} \tag{1c}$$

Where $E_{11}^{cnt}, E_{22}^{cnt}, E^{P}$ and G_{12}^{cnt}, G^{P} are the Young's moduli and shear modulus of SWCNTs and polymer matrix, respectively.

The Young's modulus of polymer matrix, under porosity, which may be a function of porosity change, are defined by (Kovacik 1999).

$$E^{p} = E_0^{p}\left(1 - P/P_c\right) \tag{2}$$

where E^p is the effective Young's modulus of porous matrix with porosity P, E_0^p is Young's modulus of matrix without porosity, P_c represent the porosity at which the effective Young's modulus becomes zero. In experimental works, either (P_c = 1) is preferably used.

Others properties in terms of mass density (ρ) and Poisson's ratio (ν), these can be defined as

$$\nu_{12} = V_{cnt}\nu_{12}^{cnt} + V_p\nu^{p} \tag{3a}$$

$$\rho = V_{cnt}\rho^{cnt} + V_p\rho^{p} \tag{3b}$$

Where V_{cnt} and V_p are the volume fractions of the CNT and porous matrix, respectively. The mass density is may also be a function of porosity change.

$$\rho^{p} = \rho_0^{p}\left(1 - P/P_c\right) \tag{4}$$

The CNT volume fraction is assumed to obey a function used for describing the uniform and symmetrical functionally graded distribution of aligned CNTs along the thickness direction of plates depicted in (Fig. 2)

UD-CNT $$V_{cnt} = V_{cnt}^{*} \tag{5a}$$

O-CNT $$V_{cnt} = 2\left(1 - 2\frac{|z|}{h}\right)V_{cnt}^{*} \tag{5b}$$

X-CNT $$V_{cnt} = 4\frac{|z|}{h}V_{cnt}^{*} \tag{5c}$$

where V_{cnt}^{*} is the volume fraction of CNTs, which can be obtained from the equation

$$V_{cnt}^{*} = \frac{W_{cnt}}{W_{cnt} + \left(\rho^{cnt}/\rho^{m}\right)\left(1 - W_{cnt}\right)} \tag{6}$$

where W_{cnt} is the mass fraction of the CNT in the nano-composite plate. In this study, the CNT efficiency parameters (η) related to the volume fraction $\left(V_{cnt}^{*}\right)$ are given from Zhu *et al.* (2012):

$\eta_1 = 0.149$ and $\eta_2 = \eta_3 = 0.934$ for the case of $V_{cnt}^{*} = 0.11$

$\eta_1 = 0.150$ and $\eta_2 = \eta_3 = 0.941$ for the case of $V_{cnt}^{*} = 0.14$

$\eta_1 = 0.149$ and $\eta_2 = \eta_3 = 1.381$ for the case of $V_{cnt}^{*} = 0.17$

3. Equations of motion

For describing the buckling behaviour of the reinforced porous plates, the displacement field of first order shear deformation theory (FSDT) is employed (Reddy 2004)

$$\begin{Bmatrix} u\left(x,y,z\right) \\ v\left(x,y,z\right) \\ w\left(x,y\right) \end{Bmatrix} = \begin{Bmatrix} u_0\left(x,y\right) \\ v_0\left(x,y\right) \\ w_0\left(x,y\right) \end{Bmatrix} + z\begin{Bmatrix} \varphi_x \\ \varphi_y \\ 0 \end{Bmatrix} \tag{7}$$

In which u_0, v_0 and w_0 are the displacements along the x, y and z directions in the mid plane of the plate and ϕx , ϕy are the bending rotation of the cross-section at any point of the reference plane if (z=0) in Eq. (7), the displacements are reduced to the classical plate theory (*CPT*).

First order shear deformation plate theory (FSDT) is studied in several works to investigate the behaviour of micro and nano structures (Fares 1999). Maryam Shokravi (2017b), analyzed the buckling of embedded laminated plates with agglomerated CNT-reinforced composite layers using FSDT and DQM. (Jafari Mehrabadi *et al.* 2012) used first order shear deformation plate theory (FSDT) to analyze the mechanical buckling of nanocomposite rectangular plate reinforced by aligned and straight single-walled carbon nanotubes.

The linear in-plane and transverse shear strains are given by

$$\begin{Bmatrix} \varepsilon_{xx} \\ \varepsilon_{yy} \\ \gamma_{xy} \\ \gamma_{xz} \\ \gamma_{yz} \end{Bmatrix} = \begin{Bmatrix} \frac{\partial u_0}{\partial x} \\ \frac{\partial v_0}{\partial y} \\ \frac{\partial u_0}{\partial y} + \frac{\partial v_0}{\partial x} \\ \varphi_x + \frac{\partial w_0}{\partial x} \\ \varphi_y + \frac{\partial w_0}{\partial y} \end{Bmatrix} + z\begin{Bmatrix} \frac{\partial \varphi_x}{\partial x} \\ \frac{\partial \varphi_y}{\partial y} \\ \left(\frac{\partial \varphi_x}{\partial y} + \frac{\partial \varphi_y}{\partial x}\right) \\ 0 \\ 0 \end{Bmatrix} \tag{8}$$

The constitutive relations is written in the form

$$\begin{Bmatrix} \sigma_{xx} \\ \sigma_{yy} \\ \sigma_{yz} \\ \sigma_{xz} \\ \sigma_{xy} \end{Bmatrix} = \begin{bmatrix} Q_{11} & Q_{12} & 0 & 0 & 0 \\ Q_{12} & Q_{22} & 0 & 0 & 0 \\ 0 & 0 & Q_{44} & 0 & 0 \\ 0 & 0 & 0 & Q_{55} & 0 \\ 0 & 0 & 0 & 0 & Q_{66} \end{bmatrix} \begin{Bmatrix} \varepsilon_{xx} \\ \varepsilon_{yy} \\ \varepsilon_{yz} \\ \gamma_{xz} \\ \gamma_{xy} \end{Bmatrix} \tag{9}$$

Where Q_{ij} are the transformed elastic constants

$$Q_{11}=\frac{E_{11}}{1-\upsilon_{12}\upsilon_{21}},Q_{22}=\frac{E_{22}}{1-\upsilon_{12}\upsilon_{21}},\quad Q_{12}=\frac{\upsilon_{21}E_{11}}{1-\upsilon_{12}\upsilon_{21}} \tag{10a}$$

$$Q_{66}=G_{12},\ Q_{55}=G_{13},\ Q_{44}=G_{23} \tag{10b}$$

The equations of motion can be derived from Hamilton's principle.

$$\int_0^t\left(\delta U+\delta V\right)dt=0 \tag{11}$$

Where δU, δV are the virtual variation of the strain energy and the virtual work done by external forces.

The expression of the virtual strain energy can be written as

$$\begin{aligned}\delta U=\int_A\{&N_{xx}\delta u_{0,x}-M_{xx}\delta\varphi_{x,x}+R_{xz}\delta\left(\varphi_x+w_{0,x}\right)+\\&N_{yy}\delta v_{0,y}+M_{yy}\delta\varphi_{y,y}+R_{yz}\delta\left(\varphi_y+w_{0,y}\right)+\\&N_{xy}\left(\delta u_{0,y}+\delta v_{0,x}\right)+M_{xy}\delta\left(\varphi_{x,y}+\varphi_{y,x}\right)\}dxdy\end{aligned} \tag{12}$$

Where stress resultants can be defined as follows

$$\left(N_{xx},N_{yy},N_{xy}\right)=\int_{-h/2}^{h/2}\left(\sigma_{xx},\sigma_{yy},\sigma_{xy}\right)dz \tag{13a}$$

$$\left(M_{xx},M_{yy},M_{xy}\right)=\int_{-h/2}^{h/2}z\left(\sigma_{xx},\sigma_{yy},\sigma_{xy}\right)dz \tag{13b}$$

$$\left(R_{xz},R_{yz}\right)=\int_{-h/2}^{h/2}\left(\sigma_{xz},\sigma_{yz}\right)dz \tag{13c}$$

By substituting Eq. (9) into Eq. (13), one obtains the stress resultants in form of material stiffness and displacement components.

$$\begin{Bmatrix}N_{xx}\\N_{yy}\\N_{xy}\end{Bmatrix}=\begin{bmatrix}A_{11}&A_{12}&0\\A_{12}&A_{22}&0\\0&0&A_{66}\end{bmatrix}\begin{Bmatrix}\frac{\partial u_0}{\partial x}\\\frac{\partial v_0}{\partial y}\\\frac{\partial u_0}{\partial y}+\frac{\partial v_0}{\partial x}\end{Bmatrix}+\begin{bmatrix}B_{11}&B_{12}&0\\B_{12}&B_{22}&0\\0&0&B_{66}\end{bmatrix}\begin{Bmatrix}\frac{\partial\phi_x}{\partial x}\\\frac{\partial\phi_y}{\partial y}\\\left(\frac{\partial\phi_x}{\partial y}+\frac{\partial\phi_y}{\partial x}\right)\end{Bmatrix} \tag{14a}$$

$$\begin{Bmatrix}M_{xx}\\M_{yy}\\M_{xy}\end{Bmatrix}=\begin{bmatrix}B_{11}&B_{12}&0\\B_{12}&B_{22}&0\\0&0&B_{66}\end{bmatrix}\begin{Bmatrix}\frac{\partial u_0}{\partial x}\\\frac{\partial v_0}{\partial y}\\\frac{\partial u_0}{\partial y}+\frac{\partial v_0}{\partial x}\end{Bmatrix}+\begin{bmatrix}C_{11}&C_{12}&0\\C_{12}&C_{22}&0\\0&0&C_{66}\end{bmatrix}\begin{Bmatrix}\frac{\partial\phi_x}{\partial x}\\\frac{\partial\phi_y}{\partial y}\\\left(\frac{\partial\phi_x}{\partial y}+\frac{\partial\phi_y}{\partial x}\right)\end{Bmatrix} \tag{14b}$$

$$\begin{Bmatrix}R_{yz}\\R_{xz}\end{Bmatrix}=\begin{bmatrix}D_{44}&0\\0&D_{55}\end{bmatrix}\begin{Bmatrix}\varphi_y+\frac{\partial w_0}{\partial y}\\\varphi_x+\frac{\partial w_0}{\partial x}\end{Bmatrix} \tag{14c}$$

where A_{ij}, B_{ij}, C_{ij}, D_{ij}, are the plate stiffness, defined by

$$\left[A_{ij},B_{ij},C_{ij}\right]=\sum_{n=1}^{3}\int_{h_n}^{h_{n+1}}Q_{ij}\left[1,z,z^2\right]dz;\qquad i,j=1,2,6 \tag{15a}$$

$$\left[D_{ij}\right]=\sum_{n=1}^{3}\beta\int_{h_n}^{h_{n+1}}Q_{ij}dz;\qquad i,j=4,5 \tag{15b}$$

Where β=5/6 is the correction factor of the shear deformation depending on the shape of the cross-section.

The principle of virtual work done by external loadings in the present case yields

$$\delta V=\int_A\left(N_x^0\frac{\partial w_0}{\partial x}\frac{\partial\delta w_0}{\partial x}+N_y^0\frac{\partial w_0}{\partial y}\frac{\partial\delta w_0}{\partial y}\right)dxdy \tag{16}$$

By substituting Eqs. (12) and (16) into Eq. (11), Then, integrating the displacement gradients by parts and setting the coefficients of δu_0, δv_0, δw_0, $\delta\varphi_x$ and $\delta\varphi_y$ to zero separately, leads to the following equations of motion.

$$\delta u_0:\frac{\partial N_{xx}}{\partial x}+\frac{\partial N_{xy}}{\partial y}=0 \tag{18a}$$

$$\delta v_0:\frac{\partial N_{yy}}{\partial y}+\frac{\partial N_{xy}}{\partial x}=0 \tag{18b}$$

$$\delta w_0:\frac{\partial R_{xz}}{\partial x}+\frac{\partial R_{yz}}{\partial y}-N_x\frac{\partial^2 w_0}{\partial x^2}-N_y\frac{\partial^2 w_0}{\partial y^2}=0 \tag{18c}$$

$$\delta\varphi_x:\frac{\partial M_{xx}}{\partial x}-R_{xz}+\frac{\partial M_{xy}}{\partial y}=0 \tag{18d}$$

$$\delta\varphi_y:\frac{\partial M_{yy}}{\partial y}-R_{yz}+\frac{\partial M_{xy}}{\partial x}=0 \tag{18e}$$

To formulate the closed-form solutions for buckling problems of simply supported CNTRC porous plates, the Navier method is employed.

$$\begin{aligned}u_0\left(x,y,t\right)&=\sum_{M=1}^{\infty}\sum_{N=1}^{\infty}U_{MN}\cos(\alpha x)\sin(\zeta y)\\v_0\left(x,y,t\right)&=\sum_{M=1}^{\infty}\sum_{N=1}^{\infty}V_{MN}\sin(\alpha x)\cos(\zeta y)\\w_0\left(x,y,t\right)&=\sum_{M=1}^{\infty}\sum_{N=1}^{\infty}W_{MN}\sin(\alpha x)\sin(\zeta y)\\\varphi_x\left(x,y,t\right)&=\sum_{M=1}^{\infty}\sum_{N=1}^{\infty}\Theta x_{MN}\cos(\alpha x)\sin(\zeta y)\\\varphi_y\left(x,y,t\right)&=\sum_{M=1}^{\infty}\sum_{N=1}^{\infty}\Theta y_{MN}\sin(\alpha x)\cos(\zeta y)\end{aligned} \tag{19}$$

Where $\alpha=\frac{M\pi}{a}$ and $\zeta=\frac{N\pi}{b}$. $i=\sqrt{-1}$

Where U_{MN}, and V_{MN}, W_{MN}, Θx_{MN} Θy_{MN} are arbitrary parameters.

Substituting the Eq. (19) into the Eq. (18), one obtains the closed-form solutions which are presented in the following operator equation.

$$\left(\begin{bmatrix} s_{11} & s_{12} & s_{13} & s_{14} & s_{15} \\ s_{12} & s_{22} & s_{23} & s_{24} & s_{25} \\ s_{13} & s_{23} & s_{33} & s_{34} & s_{35} \\ s_{14} & s_{24} & s_{34} & s_{44} & s_{45} \\ s_{15} & s_{25} & s_{35} & s_{45} & s_{55} \end{bmatrix}\right)\begin{Bmatrix} U_{MN} \\ V_{MN} \\ W_{MN} \\ \Theta_{x\,MN} \\ \Theta_{y\,MN} \end{Bmatrix} = \begin{Bmatrix} 0 \\ 0 \\ 0 \\ 0 \\ 0 \end{Bmatrix} \tag{23}$$

Where

$$\begin{aligned} &s_{11} = -A_{11}\alpha^2 + A_{66}\zeta^2,\ s_{12} = -\alpha\zeta(A_{12} + A_{66}),\ s_{13} = 0, \\ &s_{14} = -B_{11}\alpha^3 - B_{66}\zeta^2,\ s_{15} = -B_{12}\alpha\zeta - B_{66}\alpha\zeta, \\ &s_{21} = s_{12},\ s_{22} = -A_{66}\alpha^2 - A_{22}\zeta^2,\ s_{23} = 0, \\ &s_{24} = -B_{12}\alpha\zeta - B_{66}\alpha\zeta,\ s_{25} = -B_{66}\alpha^2 - B_{22}\zeta^2, \\ &s_{31} = s_{13},\ s_{32} = s_{23},\ s_{33} = -D_{55}\alpha^2 - D_{44}\zeta^2,\ s_{34} = -D_{55}\alpha, \\ &s_{35} = -D_{44}\zeta,\ s_{41} = s_{14},\ s_{42} = s_{24},\ s_{43} = s_{34}, \\ &s_{44} = -C_{11}\alpha^2 - C_{66}\zeta^2 - D_{55},\ s_{45} = -\alpha\zeta(C_{12} + C_{66}), \\ &s_{51} = s_{15},\ s_{52} = s_{25},\ s_{53} = s_{35},\ s_{54} = s_{45}, \\ &s_{55} = -D_{44} - C_{66}\alpha^2 - C_{22}\zeta^2 \end{aligned} \tag{24}$$

4. Results and discussions

In this section, numerical results of buckling behavior of porous plates are presented and discussed. The effective material characteristics of CNTRC plates employed in this work are given as follows. The PMPV is selected for the matrix of plate with 5 mm of thickness **(**Jafari Mehrabadi *et al.* 2012**)** and material properties: v^P=0.4, ρ^P=1150 kg/m^3, and E^P=2.1 *Gpa* (Wattanasakulpong 2015).

The (10, 10) SWCNTs is chosen as reinforcements with the following properties according to the study of Zhu *et al.* (2012): $v_{12}^{cnt} = 0.175$, $\rho^{cnt} = 1400 kg/m^3$, $E_{11}^{cnt} = 5.6466 TPa$, $E_{22}^{cnt} = 7.0800 TPa$, $G_{12}^{cnt} = G_{13}^{cnt} = G_{23}^{cnt} = 1.9445 TPa$.

A relationship exists between the dimensionless critical bukling loads obtained and the existing ones in the literature presented by Zhu *et al.* (2012) in Table 1.

With various reinforcement type of porous plate under axial load are considered in this table with thickness ratio of plate (*a/h*=10) and volume fraction $V_{cnt}^* = 0.11$. It is apparent from this comparison the good agreement between the results without porosity. The small variation is due to the model proposed by Zhu *et al.* (2012) which the higher-order shear deformation plate theory with an appropriate form function. In addition, there is a significant difference results for various porosity percentage for both Uniaxial and Biaxial compressive loading.

To give an idea of the effect of porosity on the critical buckling loads of square reinforced plate, a different distribution of CNTs are considered. Comparing the results, it can be seen that the dimensional critical buckling loads decrease with the increasing of porosity in uniaxial and biaxial compressive loading. The decreasing of critical loads is attributed to the effect of porosity on the rigidity of porous plate. On the other hand, the X-CNT reinforced plate has higher critical buckling loads than those of other reinforcement type for every case of porous plate. The critical buckling loads (N_{cr}) of square reinforced porous plate for UD-CNT and various FG-CNT reinforcement under uniaxial and biaxial compressive load are presented in Table 3 with different mode number. it is readily seen that the critical buckling loads increases if the mode number increases for al reinforcement type. This increasing for higher modes is attributed to the configuration form of small wavelength. However, the increasing becomes small for the increasing of porosity in the reinforced plate.

Table 4 presents critical buckling loads (N_{cr}) of square reinforced porous plate under uniaxial and biaxial compressive load with different values of carbon nanotube volume fraction for various reinforcement types. According to the results, it is clear that the critical buckling loads increases with increasing of carbon nanotube volume fraction for al reinforcement type of porous plates. It is concluded that the increasing of the carbon nanotube volume fraction V_{cnt}^*, can make the plate being stiffer.

In the current study, the (Fig. 3) below illustrates the critical buckling loads of reinforced porous plate under

Table 1 Comparisons of dimensionless critical bukling loads ($\bar{N}_{cr} = N_{cr}a^2/\pi^2 D_0$) of CNTRC square reinforced plates ($V_{cnt}^* = 0.11$, *a/h*=10, $D_0 = E^P h^3/12\left(1-(\nu^P)^2\right)$)

Uniaxial compressive load (γ_x = -1, γ_y =0)					
Reinforcement type		P =0%	P =0.05%	P =0.1%	P =0.2%
	Zhu *et al.* (2012)	Present			
UD-CNT	20.6814	20.5412	21.6275	22.8629	25.9226
X-CNT	24.2864	23.9594	24.9799	26.1089	28.7695
O-CNT	14.4990	14.9792	15.9943	17.2074	20.5145
Biaxial compressive load (γ_x = -1, γ_y =-1)					
UD-CNT	10.3407	10.2706	10.8138	11.4314	12.9613
X-CNT	12.1432	11.9797	12.4899	13.0544	14.3847
O-CNT	7.2495	7.4896	7.9971	8.6037	10.2572

Table 2 Effect of porosity on the critical buckling loads N_{cr} (KN) of CNTRC square reinforced plates ($V_{cnt}^* = 0.11$, *a/h*=10)

Uniaxial compressive load (γ_x = -1, γ_y =0)				
Reinforcement type	P =0%	P =0.05%	P =0.1%	P =0.2%
UD-CNT	2.0058	1.8479	1.6744	1.2656
X-CNT	2.3396	2.1343	1.9121	1.4046
O-CNT	1.4627	1.3666	1.2602	1.0016
Biaxial compressive load (γ_x = -1, γ_y =-1)				
UD-CNT	1.0029	0.9239	0.8372	0.6328
X-CNT	1.1698	1.0672	0.9560	0.7023
O-CNT	0.7313	0.6833	0.6301	0.5008

Table 3 Critical buckling loads N_{cr} (KN) of CNTRC square reinforced porous plates for different mode number ($V_{cnt}^{*}=0.11$, a/h=10)

		Uniaxial compressive load (γ_x = -1, γ_y =0)			Biaxial compressive load (γ_x = -1, γ_y =-1)		
(n, m)	P (%)	UD-CNT	X-CNT	O-CNT	UD-CNT	X-CNT	O-CNT
(1,1)	0	2.0058	2.3396	1.4627	1.0029	1.1698	0.7313
	0.05	1.8479	2.1343	1.3666	0.9239	1.0672	0.6823
	0.1	1.6744	1.9121	1.2602	0.8372	0.9560	0.6301
	0.2	1.2656	1.4046	1.0016	0.6328	0.7023	0.5008
(2,2)	0	4.0389	4.1714	3.8334	2.0195	2.0857	1.9167
	0.05	3.5568	3.6663	3.3916	1.7784	1.8332	1.6958
	0.1	3.0687	3.1568	2.9408	1.5344	1.5784	1.4704
	0.2	2.0738	2.1242	2.0095	1.0369	1.0621	1.0047
(3,3)	0	4.9913	5.0909	4.9069	2.4957	2.5454	2.4535
	0.05	4.3742	4.4592	4.3057	2.1871	2.2296	2.1528
	0.1	3.7552	3.8263	3.7012	1.8776	1.9131	1.8506
	0.2	2.5115	2.5563	2.4823	1.2558	1.2782	1.2412

Table 4 Critical buckling loads N_{cr} (KN) of CNTRC square reinforced porous plates for different nanotube volume fraction (a/h=10)

		Uniaxial compressive load (γ_x = -1, γ_y =0)			Biaxial compressive load (γ_x = -1, γ_y =-1)		
V_{cnt}^{*}	P (%)	UD-CNT	X-CNT	O-CNT	UD-CNT	X-CNT	O-CNT
0.11	0	2.0058	2.3396	1.4627	1.0029	1.1698	0.7313
	0.05	1.8479	2.1343	1.3666	0.9239	1.0672	0.6833
	0.1	1.6744	1.9121	1.2602	0.8372	0.9560	0.6301
	0.2	1.2656	1.4046	1.0016	0.6328	0.7023	0.5008
0.14	0	2.2600	2.6072	1.6833	1.1300	1.3036	0.8417
	0.05	2.0721	2.3671	1.5682	1.0360	1.1835	0.7841
	0.1	1.8669	2.1093	1.4404	0.9335	1.0546	0.7202
	0.2	1.3907	1.5296	1.1303	0.6954	0.7648	0.5652
0.17	0	3.1354	3.7032	2.2653	1.5677	1.8516	1.1327
	0.05	2.8922	3.3819	2.1215	1.4461	1.6910	1.0608
	0.1	2.6242	3.0333	1.9614	1.3121	1.5166	0.9807
	0.2	1.9897	2.2341	1.5684	0.9948	1.1171	0.7842

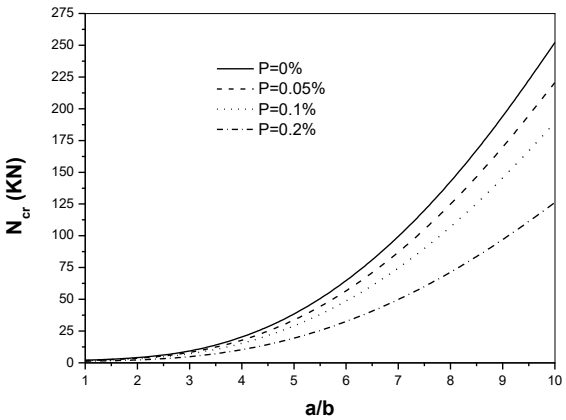

Fig. 3 Effect of aspect ratio a/b and porosity on the critical buckling loads of square reinforced porous plate under uniaxial compressive load ($V_{cnt}^{*}=0.11$)

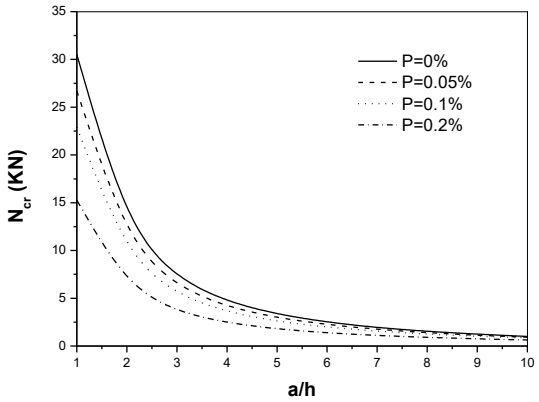

Fig. 4 Effect of thickness plate and porosity on the critical buckling loads of square reinforced porous plate under biaxial compressive load ($V_{cnt}^{*}=0.11$)

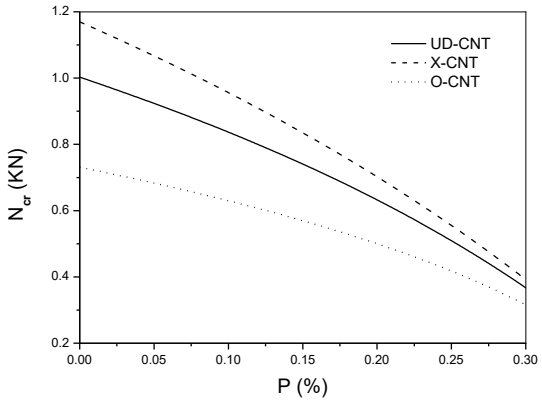

Fig. 5 Effect of porosity on the critical buckling loads of square reinforced porous plate for various reinforcement type under biaxial compressive load ($V_{cnt}^{*}=0.11$)

Uniaxial compressive load for various value of aspect ratio (a/b) to analyze the effect of porosity. it is observed that as the aspect ratio increase, the critical buckling loads increase. The augmentation of critical loads is allotted to the variation of length and width of plate. In additional, the reinforced plate without porosity has a high resistance against buckling compared to the porous plate because the latter is affected by increasing the porosity.

The (Fig. 4) illustrate the effect of aspect ratio a/h on the critical buckling loads of square reinforced porous plate. The carbon nanotube volume fraction ($V_{cnt}^{*}=0.11$) is considered in this figure. It is observed seen from (Fig. 4) that the increasing or decreasing of critical buckling loads reinforced is affected by the variation of thickness plate. Moreover, the critical buckling loads are reducing by increasing of porosity which influences the rigidity of the.

It can be seen in the current study that the rigidity of reinforced porous plate is affected by the existence of porosity which is demonstrated in (Fig. 5) with aspect ratio (a/h=10) and nanotube volume fraction ($V_{cnt}^{*}=0.11$). In these figures, it is observed that the critical buckling loads of square reinforced porous plate decrease for all case of reinforcement type.

It can be concluded that the high values estimated in X-

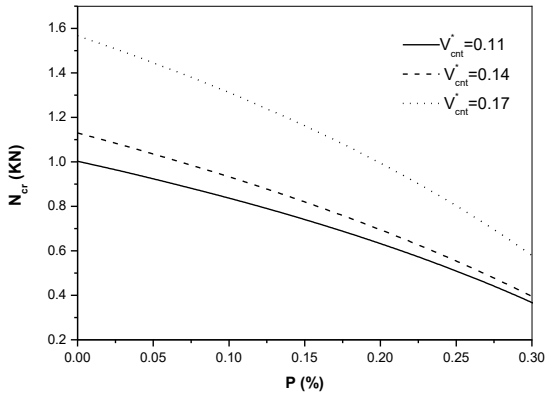

Fig. 6 Effect of porosity on the critical buckling loads of square reinforced porous plate for various carbon nanotube volume fraction under biaxial compressive load ($V^*_{cnt} = 0.11$)

CNT reinforcement is attributed to the concentration of the carbon nanotube at the top and bottom face of plate. In other hand, the range of the critical buckling loads increase with increasing of carbon nanotube volume fraction, this variation is presented in (Fig. 6) for of square reinforced porous plate under biaxial compressive load. It is concluded that the increasing of the carbon nanotube volume fraction V^*_{cnt}, can make the plate being stiffer, which requires a greater critical buckling load.

5. Conclusions

The aim of the paper is to provide a conceptual theoretical framework based on the first order shear deformation plate theory (FSDT) to studies the influence of porosity and different parameters on the critical buckling loads of reinforced porous plate. The formulations and the governing equations are solved and the values of critical buckling loads are obtained.

For this study, the results showed the dependence of critical buckling loads with the different parameters such as the porosity, volume fraction, plate thickness, aspect ratios and types of reinforcement. The results obtained from the analysis of critical buckling loads indicated that X-CNT reinforced plate has a high resistance against buckling phenomenon compared to other types of reinforcement because the concentration of the nanotubes at the top and bottom face of plate.

In terms of porosity analyses, it is found that the critical buckling loads of reinforced porous plate decrease by increasing of porosity in the polymer plate. The following conclusions were noticed from the results obtained for different parameters.

• The buckling loads decrease with the increasing of porosity in uniaxial and biaxial compressive loading.

• As the aspect ratio increase, the critical buckling loads increase.

• The increasing or decreasing of critical buckling loads reinforced is affected by the variation of thickness plate.

• It is concluded that the increasing of the carbon nanotube volume fraction V^*_{cnt}, can make the plate being stiffer, which requires a greater critical buckling load.

Acknowledgments

This research was supported by the Algerian national agency for development of university research (ANDRU) and University of Sidi Bel Abbes (UDL SBA) in Algeria.

References

Ait Amar Meziane, M., Abdelaziz, H.H. and Tounsi, A. (2014), "An efficient and simple refined theory for buckling and free vibration of exponentially graded sandwich plates under various boundary conditions", *J. Sandw. Struct. Mater.*, **16**(3), 293-318.

Ait Atmane, H., Tounsi, A. and Bernard, F. (2015), "Effect of thickness stretching and porosity on mechanical response of a functionally graded beams resting on elastic foundations", *Int. J. Mech. Mater.*, 1-14.

Ait Yahia, S., Ait Atmane, H., Houari, M.S.A. and Tounsi, A. (2015), "Wave propagation in functionally graded plates with porosities using various higher-order shear deformation plate theories", *Struct. Eng. Mech.*, **53**(6), 1143-1165.

Ajayan, P.M., Stephen, O., Colliex, C. and Trauth, D. (1994), "Aligned carbon nanotube arrays formed by cutting a polymer resin-nanotube composite", *Sci.*, **256**(5176), 1212-1214.

Arani, A.J. and Kolachi, R. (2016), "Buckling analysis of embedded concrete columns armed with carbon nanotubes", *Comput. Concrete*, **17**(5), 567-578.

Attia, A., Bousahla, A.A., Tounsi, A., Mahmoud, S.R. and Alwabli, A.S. (2018), "A refined four variable plate theory for thermoelastic analysis of FGM plates resting on variable elastic foundations", *Struct. Eng. Mech.*, **65**(4), 453-464.

Belabed, Z., Bousahla, A.A., Houari, M.S.A., Tounsi, A. and Mahmoud, S.R. (2018), "A new 3-unknown hyperbolic shear deformation theory for vibration of functionally graded sandwich plate", *Earthq. Struct.*, **14**(2), 103-115.

Belabed, Z., Houari, M.S.A., Tounsi, A., Mahmoud, S.R. and Bég, O.A. (2014), "An efficient and simple higher order shear and normal deformation theory for functionally graded material (FGM) plates", *Compos. Part B: Eng.*, **60**, 274-283.

Beldjelili, Y., Tounsi, A. and Mahmoud, S.R. (2016), "Hygrothermo-mechanical bending of S-FGM plates resting on variable elastic foundations using a four-variable trigonometric plate theory", *Smart Struct. Syst.*, **18**(4), 755-786.

Bellifa, H., Bakora, A., Tounsi, A., Bousahla, A.A. and Mahmoud, S.R. (2017b), "An efficient and simple four variable refined plate theory for buckling analysis of functionally graded plates", *Steel Compos. Struct.*, **25**(3), 257-270.

Bellifa, H., Benrahou, K.H., Bousahla, A.A., Tounsi, A. and Mahmoud, S.R. (2017a), "A nonlocal zeroth-order shear deformation theory for nonlinear postbuckling of nanobeams", *Struct. Eng. Mech.*, **62**(6), 695-702.

Bennoun, M., Houari, M.S.A. and Tounsi, A. (2016), "A novel five variable refined plate theory for vibration analysis of functionally graded sandwich plates", *Mech. Adv. Mater. Struct.*, **23**(4), 423-431.

Besseghier, A., Houari, M.S.A., Tounsi, A. and Mahmoud, S.R. (2017), "Free vibration analysis of embedded nanosize FG plates using a new nonlocal trigonometric shear deformation theory", *Smart Struct. Syst.*, **19**(6), 601-614.

Bilouei, B.S., Kolahchi, R. and Bidgoli, M.R. (2016), "Buckling of concrete columns retrofitted with nano-fiber reinforced polymer (NFRP)", *Comput. Concrete*, **18**(5), 1053-1063.

Bouazza, M., Amara, K., Zidour, M., Tounsi, A. and Adda Bedia,

E.A. (2015a), "Postbuckling analysis of functionally graded beams using hyperbolic shear deformation theory", *Rev. Informat. Eng. Appl.*, **2**(1), 1-14.

Bouazza, M., Amara, K., Zidour, M., Tounsi, A. and Adda Bedia, E.A. (2015b), "Postbuckling analysis of nanobeams using trigonometric Shear deformation theory", *Appl. Sci. Rep.*, **10**(2), 112-121.

Bouderba, B., Houari, M.S.A. and Tounsi, A. and Mahmoud, S.R. (2016), "Thermal stability of functionally graded sandwich plates using a simple shear deformation theory", *Struct. Eng. Mech.*, **58**(3), 397-422.

Bouhadra, A., Tounsi, A., Bousahla, A.A., Benyoucef, S. and Mahmoud, S.R. (2018), "Improved HSDT accounting for effect of thickness stretching in advanced composite plates", *Struct. Eng. Mech.*, **66**(1), 61-73.

Bousahla, A.A., Benyoucef, S., Tounsi, A. and Mahmoud, S.R. (2016), "On thermal stability of plates with functionally graded coefficient of thermal expansion", *Struct. Eng. Mech.*, **60**(2), 313-335.

Bousahla, A.A., Houari, M.S.A., Tounsi, A. and Adda Bedia, E.A. (2014), "A novel higher order shear and normal deformation theory based on neutral surface position for bending analysis of advanced composite plates", *Int. J. Comput. Meth.*, **11**(6), 1350082.

Chemi, A., Heireche, H., Zidour, M., Rakrak, K. and Bousahla, A.A. (2015), "Critical buckling load of chiral double-walled carbon nanotube using non-local theory elasticity", *Adv. Nano Res.*, **3**(4), 193-206.

Costa, M.L., De Almeida, S.F.M. and Rezende, M.C. (2001), "The influence of porosity on the ILSS of carbon/epoxy and carbon/bismaleimide fabric laminates", *Compos. Sci. Technol.*, **61**(14), 2101-2108.

El-Haina, F., Bakora, A., Bousahla, A.A., Tounsi, A. and Mahmoud, S.R. (2017), "A simple analytical approach for thermal buckling of thick functionally graded sandwich plates", *Struct. Eng. Mech.*, **63**(5), 585-595.

Esawi, A.M.K. and Farag, M.M. (2007), "Carbon nanotube reinforced composites: Potential and current challenges", *Mater. Des.*, **28**(9), 2394-2401.

Fares, M.E. (1999), "Non-linear bending analysis of composite laminated plates using a refined first-order theory", *Compos. Struct.*, **46**(3), 257-266.

Ghiorse, S.R. (1993), "Effect of void content on the mechanical properties of carbon/epoxy laminates", *Samp. Quarter.*, **1**, 54-59.

Hajmohammad, M.H., Zarei, M.S. and Nouri, A. (2017), "Dynamic buckling of sensor/functionally graded-carbon nanotube-reinforced laminated plates/actuator based on sinusoidal-visco-piezoelasticity theories", *J. Sandw. Struct. Mater.*, 1-33.

Han, Y. and Elliott, J. (2007), "Molecular dynamics simulations of the elastic properties of polymer/carbon nanotube composites", *Comput. Mater. Sci.*, **39**(2), 315-323.

Hebali, H., Tounsi, A., Houari, M.S.A., Bessaim, A. and Adda Bedia, E.A. (2014), "A new quasi-3D hyperbolic shear deformation theory for the static and free vibration analysis of functionally graded plates", *J. Eng. Mech.*, **140**(2), 374-383.

Iijima, S. (1991), "Helical microtubules of graphitic carbon", *Nat.*, **354**(6348), 56-58.

Iijima, S. and Ichihashi, T. (1993), "Single-shell carbon nanotubes of 1 nm diameter", *Nat.*, **363**(6430), 603.

Iwasaki, Y., Uchiyama, S., Kurita, K., Morimoto, N. and Nakabayashi, N. (2002), "A nonthrombogenic gas-permeable membrane composed of a phospholipid polymer skin film adhered to a polyethylene porous membrane", *Biomater.*, **23**(16), 3421.

Jafari Mehrabadi, S., Sobhani Aragh, B., Khoshkhahesh, V. and Taherpour, A. (2012), "Mechanical buckling of nanocomposite rectangular plate reinforced by aligned and straight single-walled carbon nanotubes", *Compos.: Part B*, **43**(4), 2031-2040.

Karami, B., Janghorban, M. and Tounsi, A. (2018a), "Variational approach for wave dispersion in anisotropic doubly-curved nanoshells based on a new nonlocal strain gradient higher order shell theory", *Thin-Wall. Struct.*, **129**, 251-264.

Karami, B., Janghorban, M. and Tounsi, A. (2018b), "Nonlocal strain gradient 3D elasticity theory for anisotropic spherical nanoparticles", *Steel Compos. Struct.*, **27**(2), 201-216.

Kolahchi, R. (2017a), "A comparative study on the bending, vibration and buckling of viscoelastic sandwich nano-plates based on different nonlocal theories using DC, HDQ and DQ methods", *Aerosp. Sci. Technol.*, **66**, 235-248.

Kolahchi, R. and Cheraghbak, A. (2017b), "Agglomeration effects on the dynamic buckling of viscoelastic microplates reinforced with SWCNTs using Bolotin method", *Nonlin. Dyn.*, **90**(1), 479-492.

Kolahchi, R. and Moniri, A.M. (2016b), "Bidgoli size-dependent sinusoidal beam model for dynamic instability of single-walled carbon nanotubes", *Appl. Math. Mech.*, **37**(2), 265-274.

Kolahchi, R., Bidgoli, M.R., Beygipoor, G. and Fakhar, M.H. (2015), "A nonlocal nonlinear analysis for buckling in embedded FG-SWCNT-reinforced microplates subjected to magnetic field", *J. Mech. Sci. Technol.*, **29**(9), 3669-3677.

Kolahchi, R., Hosseini, H. and Esmailpour, M. (2016a), "Differential cubature and quadrature Bolotin methods for dynamic stability of embedded piezoelectric nanoplates based on visco-nonlocal-piezoelasticity theories", *Compos. Struct.* **157**, 174-186.

Kolahchi, R., Keshtegar, B. and Fakhar, M.H. (2017c), "Optimization of dynamic buckling for sandwich nanocomposite plates with sensor and actuator layer based on sinusoidal-visco-piezoelasticity theories using grey wolf algorithm", *J. Sandw. Struct. Mater.*, 1-25,

Kolahchi, R., Safari, M. and Esmailpour, M. (2016c), "Dynamic stability analysis of temperature dependent functionally graded CNT-reinforced visco-plates resting on orthotropic elastomeric medium", *Compos. Struct.*, **150**, 255-265.

Kolahchi, R., Zarei, M.S., Hajmohammad, M.H. and Nouri, A. (2017d), "Wave propagation of embedded viscoelastic FG-CNT-reinforced sandwich plates integrated with sensor and actuator based on refined zigzag theory", *Int. J. Mech. Sci.*, **130**, 534-545.

Kolahchi, R., Zarei, M.S., Hajmohammad, M.H. and Oskouei, A.N. (2017a), "Visco-nonlocal-refined zigzag theories for dynamic buckling of laminated nanoplates using differential cubature-Bolotin methods", *Thin-Wall. Struct.*, **113**, 162-169.

Kolahchi, R., Zarei, M.S., Hajmohammad, M.H. and Nouri, A. (2017b), "Wave propagation of embedded viscoelastic FG-CNT-reinforced sandwich plates integrated with sensor and actuator based on refined zigzag theory", *Int. J. Mech. Sci.*, **130**, 534-545.

Kovacik, J. (1999), "Correlation between Young's modulus and porosity in porous materials", *J. Mater. Sci. Lett.*, **18**(13), 1007-1010.

Lei, Z.X., Liew, K.M. and Yu, J.L. (2013), "Buckling analysis of functionally graded carbon nanotube reinforced composite plates using the element-free kp-Ritz method", *Compos. Struct.*, **98**, 160-168.

Levkin, P.A., Svec, F. and Frechet, J.M.J. (2009), "Porous polymer coatings: A versatile approach to superhydrophobic surfaces", *Adv. Funct. Mater.*, **19**(12), 1993-1998.

Liu, L., Zhang, B.D., Wang, D.F. and Wu, Z.J. (2006), "Effects of cure cycles on void content and mechanical properties of composites laminates", *Compos. Struct.*, **73**(3), 303-309.

Madani, H., Hosseini, H. and Shokravi, M. (2016), "Differential

cubature method for vibration analysis of embedded FG-CNT-reinforced piezoelectric cylindrical shells subjected to uniform and non-uniform temperature distributions", *Steel Compos. Struct.*, **22**(4), 889-913.

Madsen, B. and Lilholt, H. (2003), "Physical properties of unidirectional plant fibre composites-an evaluation of the influence of porosity", *Compos. Sci. Technol.*, **63**(9), 1265-1272.

Mehar, K, Panda, S.K. and Mahapatra, T.R. (2017), "Thermoelastic nonlinear frequency analysis of CNT reinforced functionally graded sandwich structure", *Eur. J. Mech./A Sol.*, **65**, 384-396.

Mehar, K. and Panda, S.K. (2017), "Thermoelastic analysis of FG-CNT reinforced shear deformable composite plate under various loading", *Int. J. Comput. Meth.*, **14**(2), 1750019.

Menasria, A., Bouhadra, A., Tounsi, A., Bousahla, A.A. and Mahmoud, S.R. (2017), "A new and simple HSDT for thermal stability analysis of FG sandwich plates", *Steel Compos. Struct.*, **25**(2), 157-175.

Moradi-Dastjerdi, R. (2016), "Wave propagation in functionally graded composite cylinders reinforced by aggregated carbon nanotube", *Struct. Eng. Mech.*, **57**(3), 441-456.

Nam, Y.S. and Park, T.G. (1999), "Porous biodegradable polymeric scaffolds prepared by thermally induced phase separation", *J. Biomed. Mater. Res.*, **47**(1), 8-17.

Pradhan, S.C. and Phadikar, J.K. (2009), "Bending, buckling and vibration analyses of nonhomogeneous nanotubes using GDQ and nonlocal elasticity theory", *Struct. Eng. Mech.*, **33**(2), 193-213.

Rakrak, K., Zidour, M., Heireche, H., Bousahla, A.A. and Chemi, A. (2016), "Free vibration analysis of chiral double-walled carbon nanotube using non-local elasticity theory", *Adv. Nano Res.*, **4**(1), 31-44.

Reddy, J.N. (2004), *Mechanics of Laminated Composite Plates and Shells: Theory and Analysis*, 2nd Edition, Taylor & Francis eBooks, CRC Press.

Shafiei, H. and Setoodeh, A.R. (2017), "Nonlinear free vibration and post-buckling of FG-CNTRC beams on nonlinear foundation", *Steel Compos. Struct.*, **24**(1), 65-77.

Shen, H.S. (2009), "Nonlinear bending of functionally graded carbon nanotube reinforced composite plates in thermal environments", *Compos. Struct.*, **91**(1), 9-19.

Shokravi, M. (2017), "Buckling of sandwich plates with FG-CNT-reinforced layers resting on orthotropic elastic medium using Reddy plate theory", *Steel Compos. Struct.*, **23**(6), 623-631.

Shokravi, M. (2017), "Dynamic pull-in and pull-out analysis of viscoelastic nanoplates under electrostatic and casimir forces via sinusoidal shear deformation theory", *Microelectr. Reliab.*, **71**, 17-28

Shokravi, M. (2017a), "Buckling analysis of embedded laminated plates with agglomerated CNT-reinforced composite layers using FSDT and DQM", *Geomech. Eng.*, **12**(2), 327-346.

Shokravi, M. (2017b), "Buckling of sandwich plates with FG-CNT-reinforced layers resting on orthotropic elastic medium using Reddy plate theory", *Steel Compos. Struct.*, **23**(6), 623-631.

Shokravi, M. (2017c), "Vibration analysis of silica nanoparticles-reinforced concrete beams considering agglomeration effects", *Comput. Concrete*, **19**(3), 333-338.

Tounsi, A., Houari, M.S.A. and Bessaim, A. (2016), "A new 3-unknowns non-polynomial plate theory for buckling and vibration of functionally graded sandwich plate", *Struct. Eng. Mech.*, **60**(4), 547-565.

Tounsi, A., Houari, M.S.A., Benyoucef, S. and Adda Bedia, E.A. (2015), "A refined trigonometric shear deformation theory for thermoelastic bending of functionally graded sandwich plates", *Aerosp. Sci. Technol.*, **24**(1), 209-220.

Ulbricht, M. (2006), "Advanced functional polymer membranes", *Polym.*, **47**(7), 2217-2262.

Verdejo, R., Stampfli, R., Alvarez-Lainez, M., Mourad, S., Rodriguez-Perez, M.A., Bruhwiler, P.A. and Shaffer M. (2009), "Enhanced acoustic damping in flexible polyurethane foams filled with carbon nanotubes", *Compos. Sci. Technol.*, **69**(10), 1564-1569.

Vora, R.H., Krishnan, R.S.G., Goh, S.H. and Chung, T.S. (2001), "Synthesis and properties of designed low-k fluoro-copolyetherimides. Part 1", *Adv. Funct. Mater.*, **11**(5), 361-373.

Wan, H., Delale, F. and Shen, L. (2005), "Effect of CNT length and CNT-matrix interphase in carbon nanotube (CNT) reinforced composites", *Mech. Res. Commun.*, **32**(5), 481-489.

Wattanasakulpong, N. and Chaikittiratana, A. (2015), "Exact solutions for static and dynamic analyses of carbon nanotube-reinforced composite plates with Pasternak elastic foundation", *Appl. Math. Model.*, **39**(18), 5459-5472.

Xu, B., Arias, F.G. and Whitesides, M. (1999), "Making honeycomb microcomposites by soft lithography", *Adv. Mater.*, **11**(6), 492-495.

Zamanian, M., Kolahchi, R. and Bidgol, M.R. (2017), "Agglomeration effects on the buckling behaviour of embedded concrete columns reinforced with SiO2 nano-particles", *Wind Struct.*, **24**(1), 43-57.

Zarei, M.S., Kolahchi, R., Hajmohammad, M.H. and Maleki, M. (2017), "Seismic response of underwater fluid-conveying concrete pipes reinforced with SiO2 nanoparticles and fiber reinforced polymer (FRP) layer", *Soil Dyn. Earthq. Eng.*, **103**, 76-85.

Zhu, P., Lei, Z.X. and Liew, K.M. (2012), "Static and free vibration analyses of carbon nanotube reinforced composite plates using finite element method with first order shear deformation plate theory", *Compos. Struct.*, **94**(4), 1450-1460.

Zidi, M., Tounsi, A., Houari, M.S.A. and Bég, O.A. (2014), "Bending analysis of FGM plates under hygro-thermomechanical loading using a four variable refined plate theory", *Aerosp. Sci. Technol.*, **34**, 24-34.

Zidour, M., Benrahou, K.H., Semmah, A., Naceri, M., Belhadj, H.A., Bakhti, K. and Tounsi, A. (2012), "The thermal effect on vibration of zigzag single walled carbon nanotubes using nonlocal Timoshenko beam theory", *Comput. Mater. Sci.*, **51**(1), 252-260.

CC